SHEAR DEFORMATION AND FAILURE MODES OF GFRP REINFORCED CONCRETE BEAMS WITHOUT STIRRUPS

Monika Kaszubska[1], Renata Kotynia[2], Joaquim A. O. Barros[3]

[1] PhD student, Lodz University of Technology, Poland
[2]Associate Professor, Lodz University of Technology, Poland
[3]Full Professor, ISISE, University of Minho, Portugal

Abstract:

The various shear-transfer actions due to: aggregate interlock effect, dowel action of the flexural reinforcement, the uncracked concrete in the compressive zone and the direct strut action for the point load close to the support, may provide different crack pattern in the shear span of the concrete beams without stirrups. The aim of this paper is to investigate the shear failure mechanisms in T-shape, single span and simply supported beams exclusively reinforced with longitudinal glass fiber reinforced polymer (GFRP) bars. The research of concrete beams flexurally reinforced with GFRP bars without stirrups indicated the possibility of occurring, besides the conventional shear-compression failure mode, another type of failure governed by the loss of bond between the ordinary reinforcement and concrete. Usually the critical shear crack in RC beams without stirrups develops through the theoretical compression strut preventing a direct transfer of the shear force to the support. The main parameter affecting the crack pattern and the shear strength of the beams is the shear span to depth ratio. However, the test results presented in this paper showed the formation of an arching effect due to the bond losing between the GFRP flexural reinforcement and concrete. This failure mode revealed unexpected critical crack pattern and failure mode. Digital image correlation (DIC) technique was used to better capture and analyse the cracking process up to the formation of the shear failure crack.

Keywords: shear strength, crack pattern, GFRP bars, concrete, T-section, failure, bond, DIC.

I. Introduction

The shear force in a cracked concrete member can be transferred by number of actions: aggregate interlock effect, dowel action of the longitudinal (flexural) reinforcement, the uncracked concrete in the compressive zone, and the direct theoretical inclined strut action of point loads closest to the support (Kani 1964; Leonhardt & Walther 1962; Pruijssers 1988). The relative contribution of each mechanism changes as the load increases. Various shear-transfer actions affect in a different manner and with a varied intensity the shear concrete capacity. The shear strength transferred by these actions is highly dependent on the shape and associated kinematics of the critical shear crack. The aggregate interlock is dominant for steep critical shear cracks, whereas dowelling is dominant for flat cracks in beams with small amounts of transverse reinforcement (Campana & al. 2013).

Usually a critical shear crack in the RC beam develops through the theoretical compression strut preventing a direct transfer of the shear force to the support, leading a diagonal shear failure. The crack development through the inclined compression chord shows a very strong dependence of the shear span to depth ratio, a/d, on the shear capacity (Kani 1964). For a/d lower than 2.5 a diagonal crack does not detrimentally interfere with the inclined strut, and the shear force is transferred directly to the support. For values a/d higher than 2.5 cracks develop through the inclined struts, hence the contribution of arching action mechanism decreases, and the shear force is transferred mainly by remained beam

mechanism. However, the research conducted by Leonhardt and Walther (Leonhardt & Walther 1962) indicated another crucial effect deriving from the bond behaviour of the flexural reinforcement to concrete that has influenced the critical shear crack development.

The beams investigated by Leonhardt and Walther had the same geometry and the shear span to depth ratio equal to 2.77. The crack patterns registered in these beams are presented in Fig.1. The beam EB1, reinforced with smooth bars, has presented a load carrying capacity 94% higher than of the beam EA1 with deformed bars (the maximum shear force of EA1 and EB1 was 113 kN and 58 kN, respectively). In the beam with deformed bars (EA1) cracks developed along the shear span, and critical diagonal crack occurred almost on the line connecting the point load with the support. In the beam with smooth bars (EB1) the critical crack was almost vertical and occurred near the point load. The difference in the crack development influenced the shear strength in these beams. The diagonal crack in the EA1 beam, which developed through the inclined compression strut, caused that the shear force was transferred to the support due to aggregate interlock mechanism, which was less efficient than the direct strut action. In the specimen EB1, due to lower bar-to-concrete bond strength, only a limited part of the inclined crack developed through the theoretical inclined strut, which enabled direct transfer shear force to the support and significantly increased the load capacity of the member (Muttoni & Ruiz 2008).

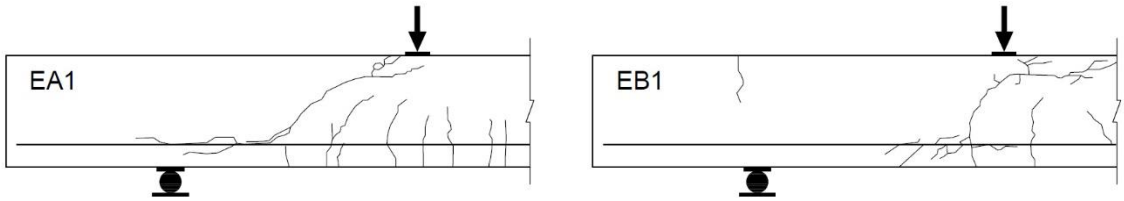

Fig. 1 The crack pattern in beams tested by Leonhardt and Walther 1962, and theoretical strut position.

A similar phenomenon based on two different failure modes (shear-compression failure and failure governed by the loss of bond) was observed in an experimental research conducted on the GFRP reinforced concrete beams at the Laboratory of Concrete Structures in the Lodz University of Technology, which is discussed in this paper. The aim of the investigation was to analyze the critical shear crack development, failure modes and the ultimate loads. For a deeper analysis of the cracking pattern during the failure process, a digital measurement based on photogrammetry tools was carried out.

II. Details of tested beams

The selected twelve RC beams presented in this paper belong to an extensive experimental research program consisting of two series of T-shape cross section RC beams (b_f = 400 mm, b_w = 150 mm, h_f = 60 mm, h_f = 360 mm, h_{tot} = 400 mm, Fig. 2), single span and simply supported with a clear span of 1800 mm, tested in three-point monotonic loading configuration. The first investigated parameter was the influence of the flexural reinforcement ratio, ρ_l, on the beam's shear capacity, by considering different number of bars per layer, number of layers, and bar diameter, namely: $\rho_l \approx 1.0\%$, $\approx 1.4\%$, and $\approx 1.8\%$; bar's diameters of 12, 16, and 18 mm.

The second investigated parameter was planned the concrete compressive strength (f_{cm}). In the series I the concrete strength class was C25/30 (f_{cm}=31.7 MPa), while in the series II it was expected to have a concrete of strength class C50/60. Unfortunately, the concrete ordered for the second series has presented an average compressive strength of 35.9 MPa, much lower than expected, but this situation was only verified when testing the beams of this series. Despite the influence of f_{cm} can not be investigated as initially planned, the results of both series are presented and discussed in this paper. Since the

composition for the concrete of series II is not available, Table 1 only presents the composition of concrete of series I beams.

Table 1. Concrete composition of the beams of series I.

Components	Quantity (kg/m^3)	Ratio (%)
Sand 0/2	970	42.33
Crushed stone 2/8	860	37.53
Water	205	8.94
CEM I 42.5 Rudniki CEMEX	255	11.13
Plasticizer BV-Cemex Admixtures	1.8	0.07
Total	∑=2291.8	100.00

The third investigated parameter was the concrete cover thickness, having been adopted the values of 15 mm and 35 mm. The summary of twelve tested beams is presented in Table 2.

Table 2. Details of the tested beams.

Beams	Series	f_{cm} (MPa)	A_l (mm^2)	ρ_l (%)	d (mm)	a/d (-)
G-512-35-15	II	36.02	565	0.99	379	2.90
G-512-30-15	I	30.20				
G-512-35-35	II	34.95		1.05	359	3.06
G-512-30-35	I	28.80				
G-318-35-35	II	34.95	763	1.43	356	3.09
G-318-30-35	I	30.50				
G-318-30-15	I	28.80		1.35	376	2.93
G-318-35-15	II	37.05				
G-418-35-15	II	35.00	1018	1.80	376	2.93
G-418-30-15	I	28.80				
G-418-35-35	II	35.00		1.91	356	3.09
G-418-30-35	I	30.20				

2.1 Reinforcement

For the beam's designation the following acronym was adopted, G-X#-Y-Z, where G means the flexural GFRP bars, X is the number of bars of # diameter (in mm), Y in series I represents the average compressive strength for the concrete on the cubic specimens, while in series II the average compressive strength for the concrete on the cylinder specimens, and Z is the concrete cover thickness. For instance, G-512-35-35 is a beam flexurally reinforced with a layer of 5 bars of 12 mm diameter, belonging to series II with a concrete cover thickness of 35 mm. The bottom straight GFRP bars were anchored by embedding the bars into a steel box (Fig.2) filled with an epoxy resin (Sikadur 30, modulus of elasticity in compression and tension of 11.2 GPa and 9.6 GPa, respectively).

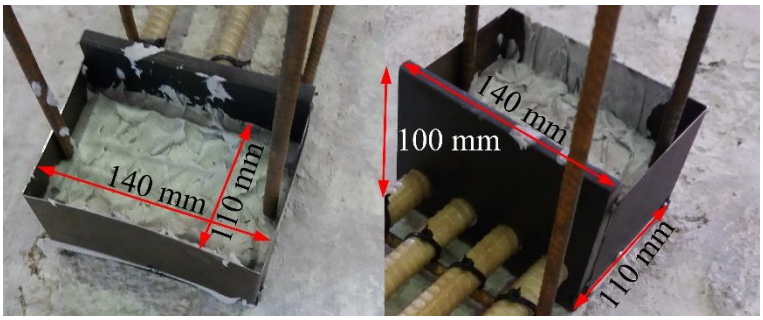

Fig. 2 The anchorage of bottom bars**.**

The top longitudinal reinforcement of all beams consisted of two straight GFRP bars of 10 mm diameter, maintained in their aimed position by using transversal short steel bars of 6 mm diameter at 210 mm spacing, located in the flange (Fig.2).

There were no stirrups in the largest shear span. Only the shortest shear span was reinforced with closed steel stirrups of 8 mm diameter at 150 / 90 mm spacing in beams with concrete cover thickness of 15 mm, and at 130 / 90 mm spacing in beams with concrete cover thickness of 35 mm. Apart from the stirrups, steel bent bars of 14 mm diameter were used to avoid shear failure in the shortest shear span (Fig. 3).

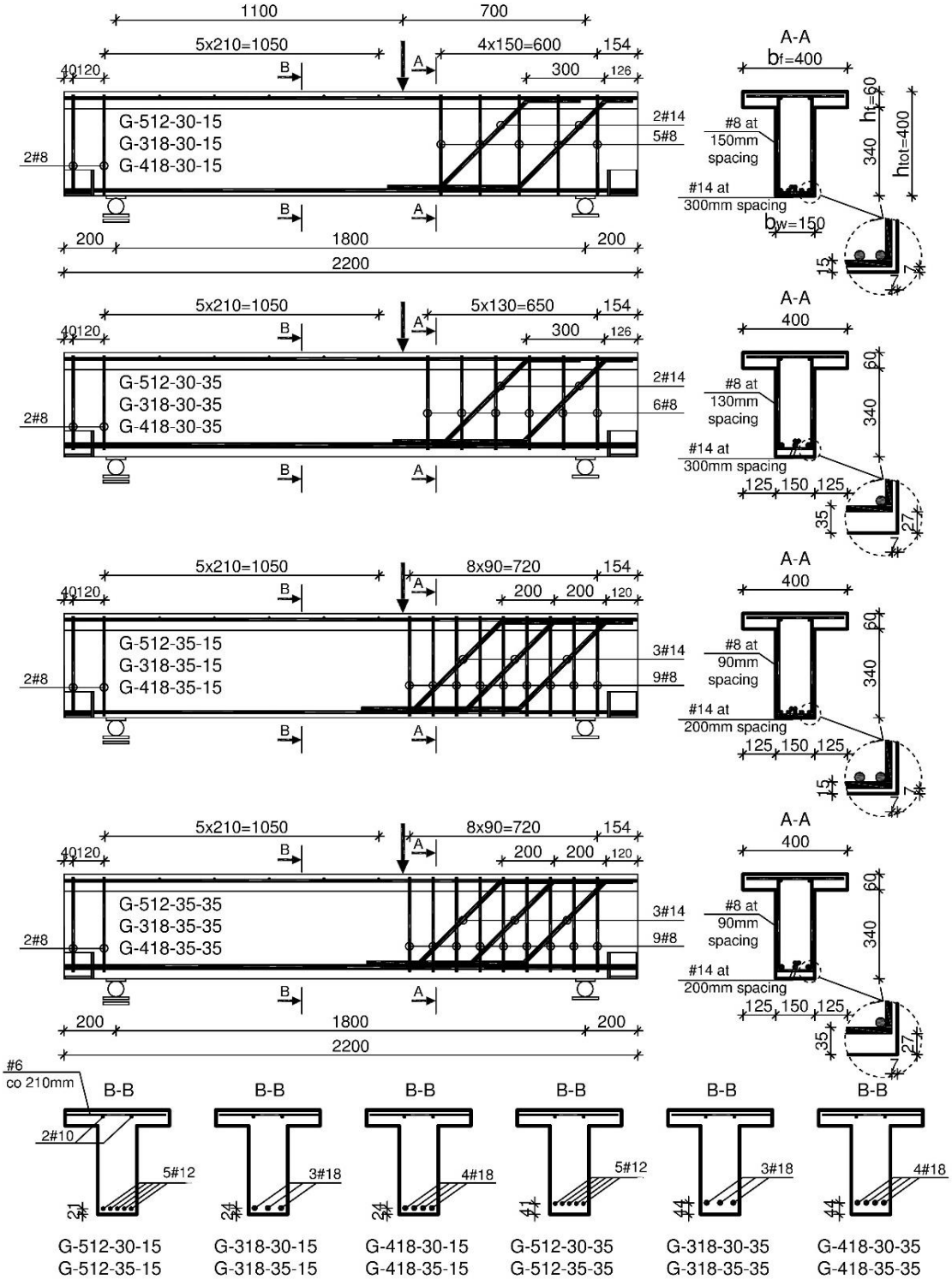

Fig. 3 Geometry and reinforcement details of the tested beams (dimensions in mm).

2.2 Test set-up

The beams were simply supported on two steel supports, one providing free rotation and beam's axial displacement, and the other with only free rotation movement (Fig. 4). The load was applied under displacement control at 10 μm/s by using T-cross section steel profile to distribute the applied load along the width of the flange (contacted area of 10 mm × 400 mm). Concrete axial strains were evaluated by using displacement transducers (LVDTs) disposed in the middle depth of one of the lateral faces of the beam's flange (number 1 to 4), and LVDTs positioned 30 mm above the bottom beam's surface (number 5 to 8). Vertical displacements were registered by eight LVDTs of 20 mm stroke and 0.1 mm accuracy (number 22 to 29) mounted on an independent steel frame (Fig. 4).

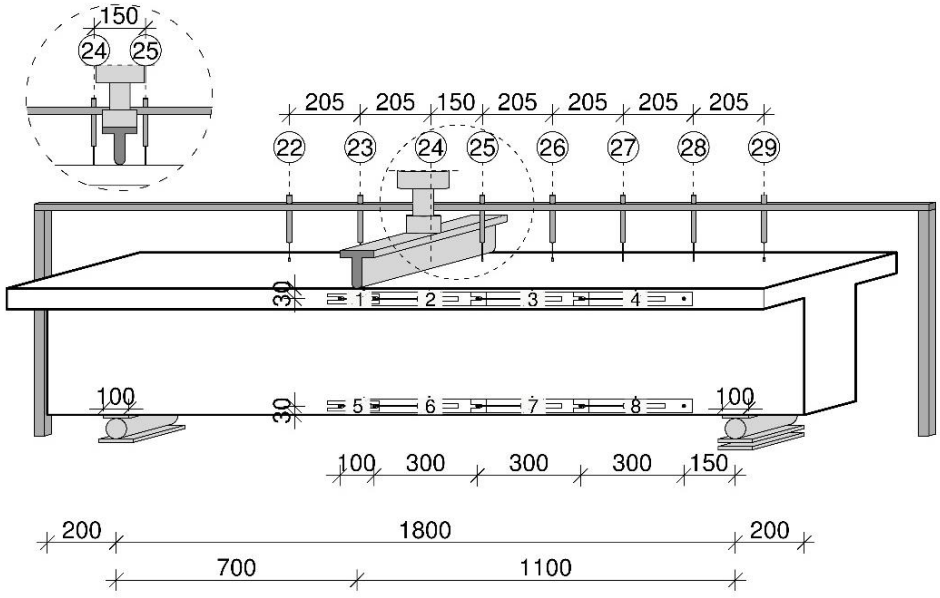

Fig. 4 Schematic representation of LVDTs (dimensions in mm).

The digital image correlation (DIC) system was used to help on the interpretation of the cracking process of the tested beams. The information from DIC is obtained by comparing digital photographs of a component or test piece at different stages of deformation. By tracking blocks of pixels, the system can measure surface displacement and build up the full 2D and 3D deformation vector fields and maps of concrete strains. The photogrammetric technique used in this research was prepared for 3D measurements using two cameras with a focal length of 50 mm and a resolution of 4 megapixels. Pictures were taken at 1 Hz frequency. The registered area of concrete was 500 mm wide, 340 mm high in the beams of series I and 1100 mm wide and 400 mm high in the beams of series II. This area was located in the mid-span of the shear region (indicated by a square at dashed line in Fig. 5).

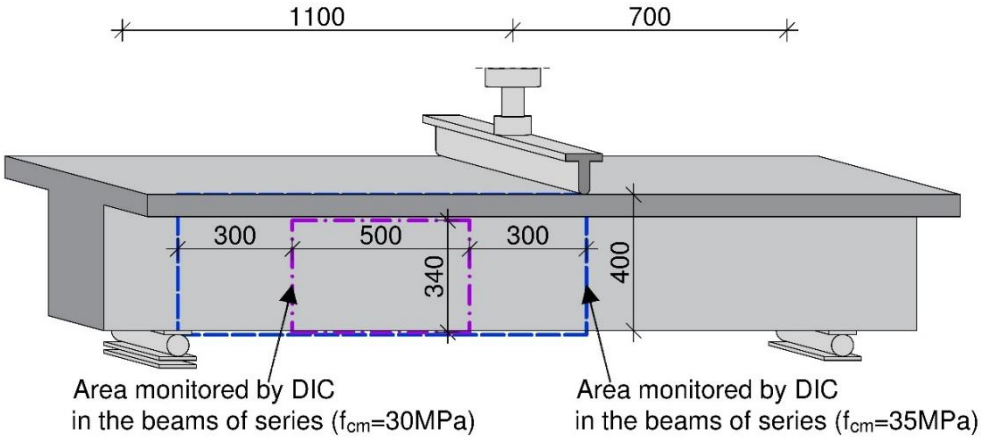

Fig. 5 The area monitored by DIC in beams of series I (f_{cm}=30 MPa) and II (f_{cm}=35 MPa) (dimensions in mm).

2.3 Properties of the materials

2.3.1 Concrete

The strength properties of concrete were determined according to EN 206-1 standard (European Committee for Standardization (CEN) 2013). The average cylinder concrete compressive strength, f_{cm}, in the beams of series I (obtained on 15 specimens) was 31.7 MPa (COV=8%), the average modulus of elasticity, E_{cm}, was 26.7 GPa (COV=6%), while the average splitting tensile strength, $f_{ct,spl}$ (from Brazilian type test), was 2.9 MPa (COV=8%). In the beams of series II, an f_{cm}=35.9 MPa (obtained on 11 specimens, COV=4%), E_{cm}=25.8 GPa (COV=3%), and $f_{ct,spl}$=3.4 MPa (COV=7%) were obtained.

2.3.2 GFRP bars

The relevant tensile properties of the GFRP reinforcement were determined from the experimental tests carried out on 15 specimens according to ISO Standard 10406-1 (International Organization for Standardization (ISO) 2015). The average value of the modulus of elasticity and the tensile strength registered in these tests were 50.5 GPa (COV=1.6%) and 1091 MPa (COV=10.7%), respectively.

III. Test results

The main obtained results are presented in Table 3. In order to take into account the different flexural reinforcement depth on the shear capacity of the beams, the concept of average shear stress ($\tau=V/(b_w d)$ was used, where V is the shear force in the monitored span. In this table δ_{Fmax} is the average vertical displacement registered by two LVDTs No 24 and 25 (Fig. 3) at the maximum load.

Table 3. Test results

Beams / Series	V_{max} (kN)	τ_{max} (MPa)	δ_{Fmax} (mm)	Failure mode
G-512-35-15* / II	29.66	0.52	0.8	B
G-512-30-15 / I	34.27	0.60	4.9	SC
G-512-35-35 / II	60.27	1.12	10.4	B
G-512-30-35 / I	32.47	0.60	3.5	SC
G-318-35-35 / II	46.04	0.86	4.9	B
G-318-30-15 / I	38.57	0.68	2.6	SC
G-318-35-15 / II	33.76	0.60	3.2	SC
G-318-30-35 / I	34.42	0.64	2.6	SC
G-418-35-15 / II	50.03	0.89	7.2	B
G-418-30-15 / I	38.14	0.68	2.4	SC
G-418-35-35 / II	35.14	0.66	2.1	SC
G-418-30-35 / I	39.41	0.74	2.6	SC
* Test was stopped due to the formation of extensive horizontal cracks of large width; SC-shear compression failure; B- bond failure of GFRP bars to concrete				

3.1 Cracking patterns and failure modes

In almost all beams the first flexural cracks occurred in the beam mid-span. More flexural cracks have developed during the load process, and at a shear stress level of about 0.59-0.87 τ_{max} a diagonal crack appeared in the shear region. In all six beams of series I and in two of the six beams of series II failure proceeded according to the typical shear - failure observed in other research by (Cavagnis, Fernández Ruiz & Muttoni 2015; Marí & al. 2015).

However, in four of the six beams of series II, the loss of bond between the flexural reinforcement and concrete has occurred, a type of failure model not observed in the beams already tested in the scope of this research program. The cracking pattern in these four beams was completely different than in in the rest of beams failed due to general shear-compression (compare Figures 6-11). These beams reached much higher maximum shear force V_{max} than the beams of series I (see Table 3).

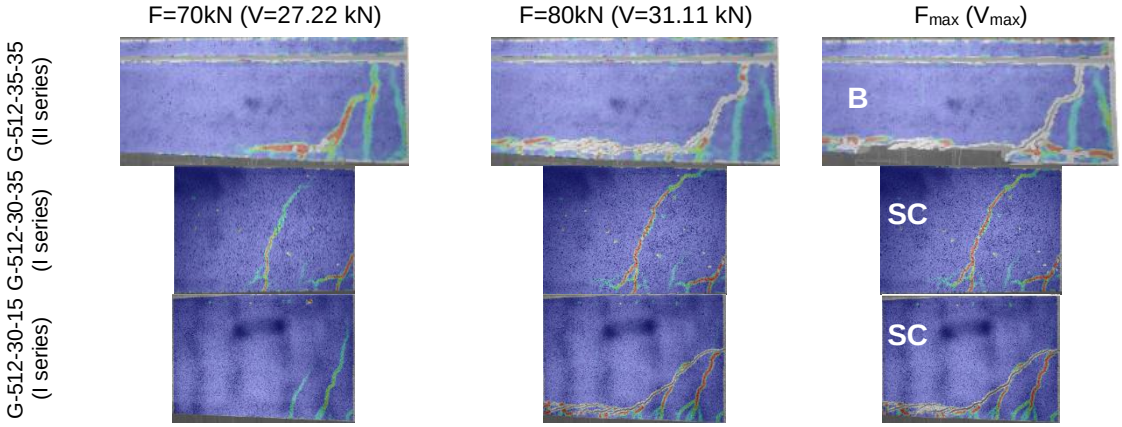

Fig. 6 Crack development in beams with reinforcement ratio ~1%.

Moreover, even though the concrete compressive strength of the beams of series II was higher than the beams of series I, the maximum shear force of two beams G-318-35-15 / II and G-418-35-35 / II, which failed due to shear-compression (SC) in series II, was lower than the maximum shear force of corresponding two beams in series I (e.g. V_{max} = 38.57 kN for G-318-30-15 beam and V_{max} = 33.76 kN for G-318-35-15 beam).

The first flexural crack appeared close to the loaded section (in the bending moment region) in the beams that failed due to shear-compression (G-512-30-15, G-512-35-35, G-512-30-35, G-318-30-15, G-318-35-15, G-318-30-35, G-418-30-15, G-418-30-35, G418-35-35). By increasing the load, the next cracks formed between the previous ones, in the zone close to the flexural reinforcement, as a consequence of the bond stress transfer between this reinforcement and surrounding concrete. Then, the inclined crack propagated towards the flexural cracks, finally forming the critical shear crack at distance 0.57-1.60 d from the support (Fig. 9-11). Development of one of these critical shear cracks into the shear failure crack was governed by two mechanisms in the extremities of this crack: in the top extremity the crack progressed to the load point due to the relatively high influence of both shear and bending moment in this region; in the bottom extremity, the shear failure crack progressed along the interface between flexural reinforcement and surrounding concrete (Figures 6-8, beams signed SC).

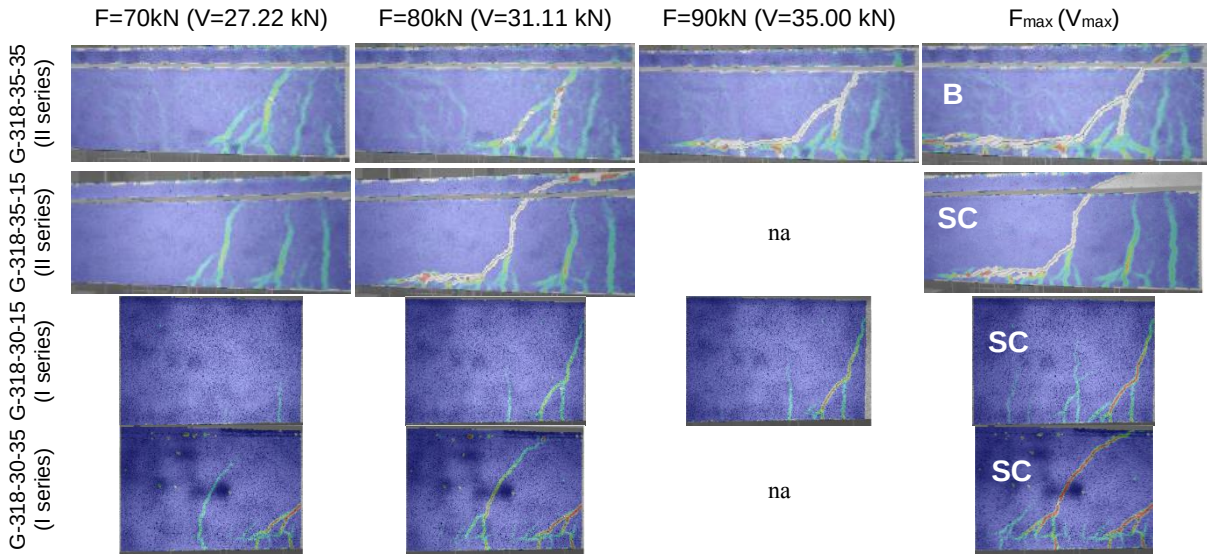

Fig. 7 Crack development in beams with reinforcement ratio ~1.4%

When the primary flexural crack reached the flange, its inclination became almost flat progressing into the web-flange interface of the T-cross section. Finally, this crack propagated to the loading zone with a higher inclination, crossing the whole flange. Due to the shear sliding between the two concrete blocks the shear failure crack divides the beam in its shear span, and considering the shear contribution of the reinforcement located in the flange, a negative bending moment appeared at the top flange, which behaved like a cantilever (Kaszubska & al. 2017). This shear-compression failure was observed in all beams of the series I and in only two beams of the series II. The critical shear crack in these beams crossed the theoretical inclined compression strut of beam and interrupted a direct transfer of the shear force to the support. According to (Muttoni & Ruiz, 2008) in this case the shear force was mainly transferred by an elbow-shaped strut and straight strut that develop do to the aggregate interlock action in the critical shear crack. A development of an elbow-shaped strut deviated the compression strut leading to avoid the shear cracks propagation. This new shear-carrying mechanism (due to the arching

action) depends on the crack pattern and the aggregate size that probably was smaller in the beams of series II comparing to the beams of series I (based on the visual inspection of the concrete specimens tested for the characterization of its properties).

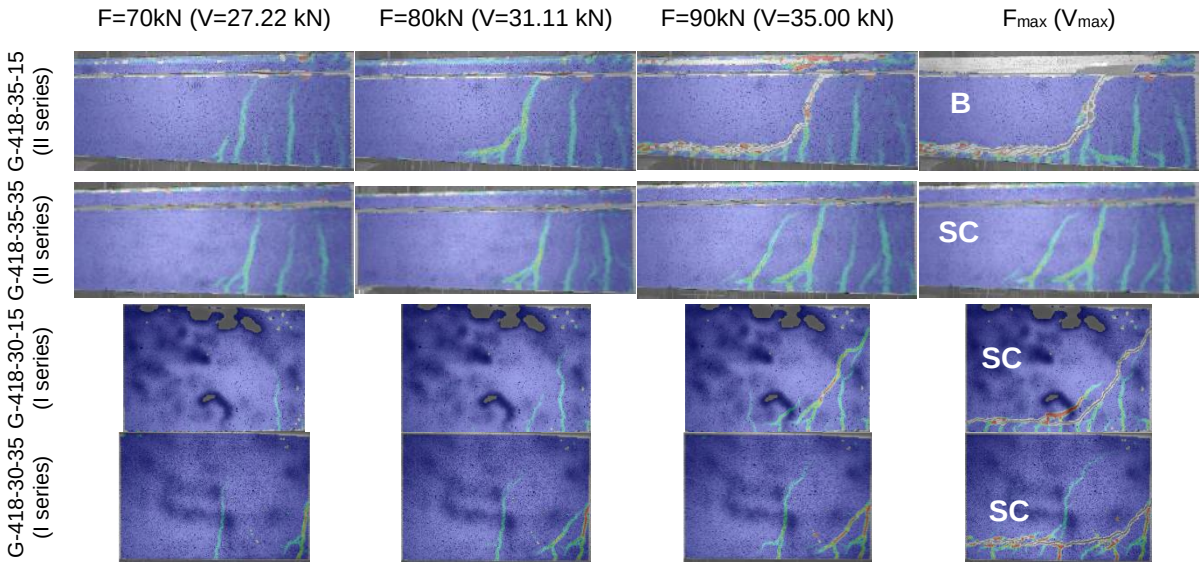

Fig. 8 Crack development in beams with reinforcement ratio ~1.8%

Completely different failure occurred in four beams of series II (G-512-35-15, G-512-35-35, G-418-35-15 and G-318-35-35), proceeded by an unexpected crack pattern comparing to the previous beams failed due to shear-compression (SC). In two beams of the series II (f_{cm}=35 MPa) there were a clear bond loss of the GFRP bars to the concrete with visible detachment of the bottom concrete cover. Under initial loading of the beam G-512-35-15, the typical flexural cracks appeared close to the point load. Then the primary crack developed in a horizontal direction at the level of the bottom reinforcement leading the loss of bond between the bottom bars to the surrounding concrete along to the flexural GFRP reinforcement (out of the recorded DIC area, Fig. 5). Due to concerns about this new failure mode (never observed in the previous beams) and concerns about damage of the installed LVDT gauges, the test was stopped at the level of load 29.66 kN without any evidence of being close to its collapse. This is why the beam G-512-35-15 was excluded from further analysis. Therefore, when the similar crack pattern was recorded in the next beam G-512-35-35, the test was continued until the evident failure confirmed by the load decreasing. The beam G-512-35-35 initially cracked in flexure with the almost vertical cracks, which after the bond loosing of the flexural reinforcement changed inclination for horizontal and developed to the support. This horizontal crack led to detachment of the concrete cover. However, in the opposite shortest span (shear reinforced) extensive shear cracking has occurred. The short horizontal crack appeared at the interface between the web and the flange, then the crack changed for the vertical one crossing the flange under the point load. The beam G-512-35-35 reached much higher ultimate load than the other beams of similar reinforcement ratio (compare Table 3).

Four of the six beams of series II, which failed due to the loss of bond between the flexural GFRP reinforcement and concrete prevented the inclined cracking through the theoretical inclined strut (Figures 6-8), that was observed in RC beams reinforced with steel (Muttoni & Ruiz 2008).

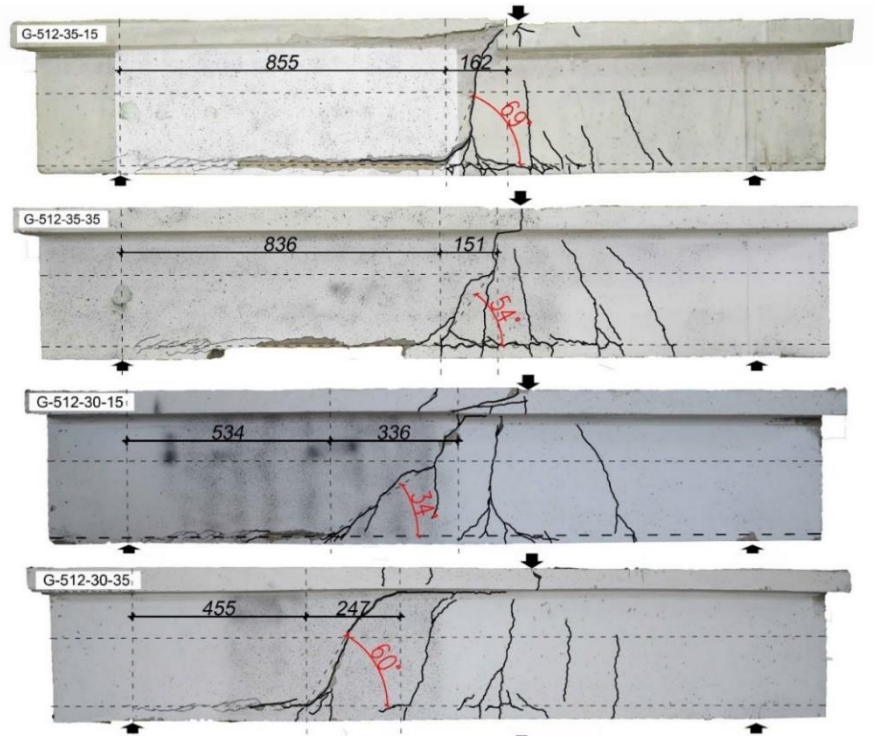

Fig. 9 The crack pattern beams with reinforcement ratio ~1%.

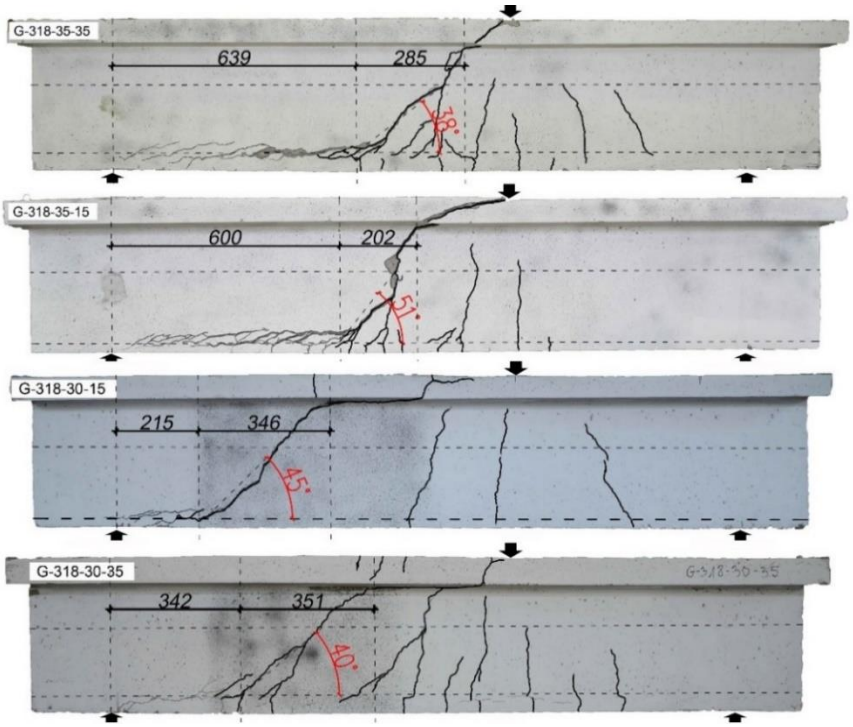

Fig. 10 The crack pattern beams with reinforcement ratio ~1.4%.

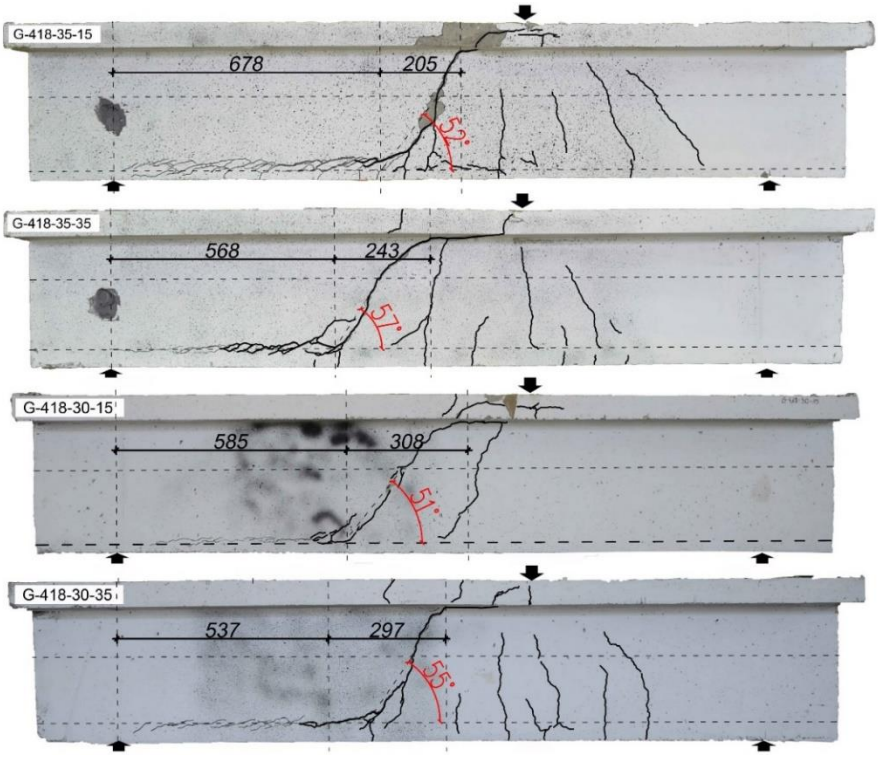

Fig. 11 The crack pattern beams with reinforcement ratio ~1.8%.

3.2 Capacity

Two beams in the series II, which failed in shear-compression, reached the lower shear capacity in relation to the analogous beams in the series I, despite a slightly higher capacity was expected due to the higher compressive concrete strength (Table 3). Probably the decrease in the shear strength was caused by a reduction of the aggregate interlock action due to smaller aggregate size detected in the concrete of these beams.

In spite of the bond losing between the flexural reinforcement and concrete in three of the six beams of series II (G-512-35-35, G-418-35-15 and G-318-35-35) they reached the higher capacity than the corresponding members of series I, which failed due to the the typical shear-compression failure. The shear forces in the tested support region, corresponding to the calculated load bearing capacity was equal of 150.30 kN for G-512-35-35, 166.28 kN for G-318-35-35 and 196.60 kN for G-418-35-15, which ensures high protection against the flexural failure.

A comparison of the maximum shear stress $\tau_{max} = V_{max}/(b_w d)$ reached in three beams, which failed due to the loss of bond between the GFRP reinforcement and concrete (black bar with red border charts in Fig. 12) with analogous beams failed in shear-compression (grey bar charts in Fig. 12), indicate the significant increase in the capacity of these three beams in comparison to the rest of beams with the same flexural reinforcement ratio, which failed due to the typical shear-compression e.g.: 86% strength increase for beams with ρ_l~1%; between 26% and 34% for beams with ρ_l ~1.4% and between 20% and 35% for beams with ρ_l ~ 1.8%. The biggest difference in the shear capacity occurred in the beams with

the lowest reinforcement ratio (ρ_l~1%), where the theoretical compression strut was the latest exposed to the critical diagonal shear crack (compare Fig. 12).

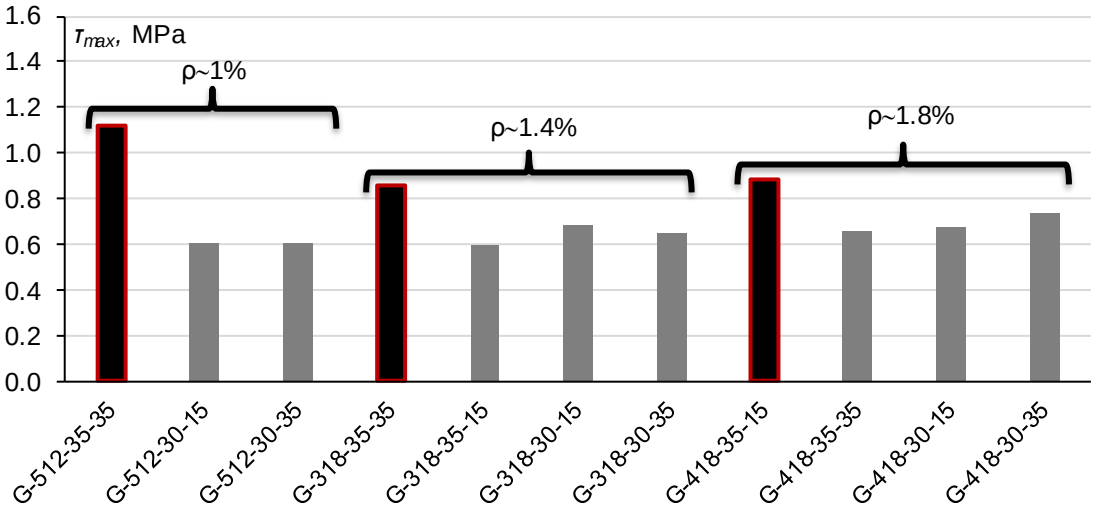

Fig.12. The maximum shear stress τ_{max} of the tested beams**.**

3.3 Deflection

The shear stress charts in function of mean vertical displacement (τ-δ) registered by LVDTs No 24 and 25 are presented in Fig. 13, 14 and 15. The beams G-512-35-35, G-418-35-15 and G-318-35-35 (with the arching action) failed due to the loss of bond indicate a similar bi-linear behavior to the corresponding beams failed due to the shear-compression (compare Fig. 9, 10 and 11). However, after a limit of the shear strength in the beams failed in shear-compression, the arching action caused the further shear stress increase almost linear until failure.

The higher capacity of these three beams led to an increase in the deflection at the ultimate load. The significant increase in the average deflection δ_{Fmax} was observed in the beams with the reinforcement ratio ρ_l~1% and ρ_l~1.8% (114-201% and 200-326%, respectively, Table 3).

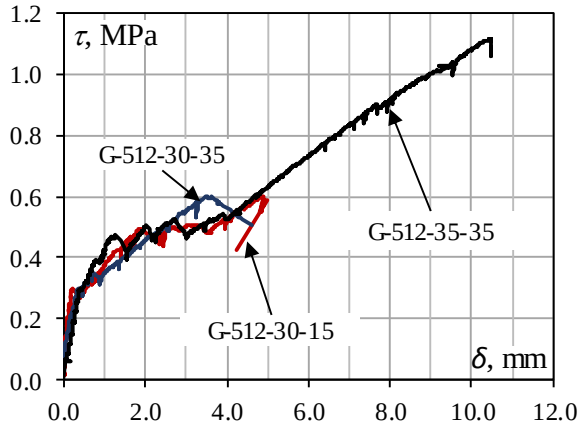

Fig. 13 The average deflection in beams with reinforcement ratio ~1%.

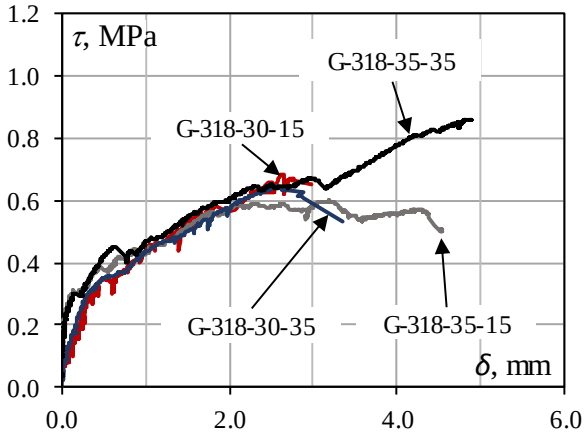

Fig. 14 The average deflection in beams with reinforcement ratio ~1.4%.

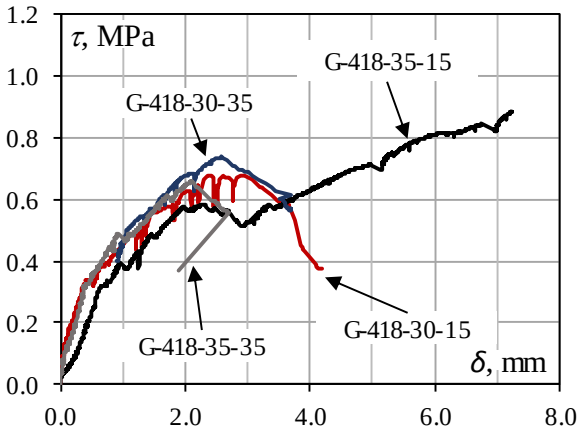

Fig. 15 The average deflection in beams with reinforcement ratio ~1.8 %.

IV. Conclusions

The paper presents test results of T-section, GFRP flexurally reinforced beams without stirrups that revealed two failure modes: typical shear-compression failure and bond losing between GFRP bars and concrete. From the experimental tests the following conclusions can be drawn:

- The load carrying capacity of beams was highly dependent on the shape and localization of the critical shear crack;
- The concrete composed of smaller aggregate (in the beams of series II) caused bond loss between GFRP bars and concrete in the maximum bending region forming the arching action and preventing inclined cracking in the shear span;
- The arching action in the beams which failed due to bond loos significantly increased the strength of the beams (from 20% for the typical shear failure to 86% for the bond losing failure);
- The beams failed due to the loss of bond indicated similar shear stress-deflection curves to these in the beams failed due to shear-compression.

Acknowledgement

The authors gratefully acknowledge the ComRebars Company who supplied the GFRP reinforcement for the experimental tests.

References

Campana, S., Fernández Ruiz, M., Anastasi, A. & Muttoni, A. (2013), Analysis of Shear-Transfer Actions on One-Way RC Members Based on Measured Cracking Pattern and Failure Kinematics. Magazine of Concrete Research, Vol. 65, No. 6, pp. 386–404.

Cavagnis, F., Fernández Ruiz, M. & Muttoni, A. (2015), Shear Failures in Reinforced Concrete Members without Transverse Reinforcement: An Analysis of the Critical Shear Crack Development on the Basis of Test Results. Engineering Structures, No. 10, pp. 157–173.

European Committee for Standardization (CEN). (2013), EN 206 2013. Concrete — Specification, Performance, Production and Conformity. European Standard.

International Organization for Standardization (ISO). (2015). 10406-1. Fibre-Reinforced Polymer (FRP) Reinforcement of Concrete Test Methods Part 1: FRP Bars and Grids.

Kani, G. (1964), The Riddle of Shear Failure and Its Solution. ACI Journal Proceedings, Vol. 61, No. 4, pp. 441–468.

Kaszubska, M., Kotynia, R., Barros, J.A.O. & Baghi H. (2017), Shear Behavior of Concrete Beams Reinforced Exclusively with Longitudinal Glass Fiber Reinforced Polymer Bars: Experimental Research. Structural Concrete, Vol. 19, No. 1, pp. 152–161.

Leonhardt, F., & Walther, R. (1962), Shear Tests on Beams With and Without Shear Reinforcement. Deutscher Ausschuss Für Stahlbeton, No. 151, 83p.

Marí, A., Bairán, J., Cladera, A., Oller E. & Ribas, C. (2015), Shear-Flexural Strength Mechanical Model for the Design and Assessment of Reinforced Concrete Beams. Structure and Infrastructure Engineering, No. 11, pp. 1399–1419.

Muttoni, A. & Fernández Ruiz, M. (2008), Shear Strength of Members without Transverse Reinforcement as Function of Critical Shear Crack Width. ACI Structural Journal Vol. 105, No. 2, pp. 163–172.

Pruijssers, A. (1988), Aggregate Interlock and Dowel Action under Monotonic and Cyclic Loading.Delft University of Technology.